Journal of the Korean Institute of Illuminating and Electrical Installation Engineers Vol. 21, No.9, pp. 64~75 November 2007 (21-9-10)

A Study of the PV System for Optimum Design Methods With Loss Parameter Compensation

Kang-Yeon Lee* · Moon-Han Choi · Youn-Ok Choi · Byeong-Ho Joeng · Geum-Bae Cho**

Abstract

Photovoltaic systems utilize the infinite clean energy of the sun, without creating any air pollution or noise and mechanical vibration. A PV system operates without the need of fuel, rotation surfaces, high temperatures or high pressures. It is therefore to do maintain and simple to install as well as having a long life cycle. The global market for PV systems continues to grow rapidly by 30[%] per year.

This paper suggests a new design method for the PV system installation that will allow to the improvement of system efficiency. This method is in accordance with the loss parameter compensation method designed for the PV systems and investigated through simulation and practical experimentation. It was applied to an interconnected 10[kW] grid PV system and was demonstrated in the field. Features such as solar array, PCS, system efficiency, performance and stability were considered. Through the proposed optimal parameter design method, the features of the system were studied, and the 10[kW] PV system was demonstrated and analyzed.

Key Words : Grid connected PV system, Optimum design, Field test

1. Introduction

A PV system is divided into a grid-linked power generation system that transmits and stores the surplus power produced during the daytime to the power system, and an independent power generation system that stores this power in storage batteries.

Owing to system link technology, the establishment of system protection technology standards, and the development of inverter technology, the continuing development of PV systems is focusing on grid-linked power generation systems through conversion into large scale and high efficiency capacity. The distribution rate of PV systems is increasing rapidly through the activation of distribution technology as compared with other new renewable energy fields. The design for performance stabilization and standards of installations are keeping pace with this demand, and a variety of demonstrations and field validation tests are being performed[1-4].

* Main author : Adjunct, Department of Electrical Engineering, Chosun University
** Corresponding author : Professor, Department of Electrical Engineering, Chosun University
Tel : +82-62-230-7031, Fax : +82-62-230-7020
E-mail : space122@hanmail.net
Date of submit : 2007. 8. 23
First assessment : 2007. 8. 24
Completion of assessment : 2007. 9. 11

In light of this trend, a study of the design method and performance index of a PV system was conducted along with a detailed technical review for loss factors of this design. Also, to ensure optimal design, simulation of the system was conducted by means of external environmental conditions, an array arrangement of solar cells, shadow effect, voltage drop, and design technology following the azimuth and tilt angle for optimum design, which can improve efficiency of the PV system. These results were applied to a 10[kW] grid-linked PV system to evaluate performance. Operational characteristics and system stability as related to the characteristics of solar cell array, PCS characteristics, system efficiency and performance were studied through this demonstration. Design technology to improve the efficiency of a grid-linked 10[kW] PV system is suggested by analyzing the results.

2. Design method of the PV system

2.1 Design method of the PV system

When designing power generation equipment, output conditions are determined depending upon the required load power. Input energy is typically designed as shown in Fig. 1(a). Since photovoltaic generation requires solar energy, which has a limited output per unit area, as input, this precondition may not in fact be possible.

Since the size (capacity) of electrical equipment is determined by wattage, order is then determined over short-term and long-term factors as shown in Fig. 1(b) in the design of a PV system. Since input is irregular and variable depending upon the performance of the solar cell and the surrounding environment such asinsolation rate and temperature, the system design should take into consideration these factors[5].

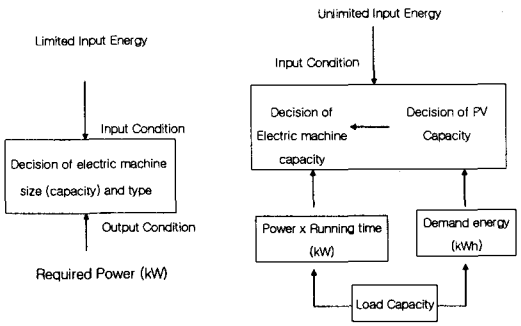

(a) System design of general electric machine (b) System design of PV system

Fig. 1. Design difference of an equipment generator and PV generator

The solar energy received by solar cells is a loss parameter due to the reduced efficiency or output included in the course through which electrical energy converted by the photoelectric elements is supplied to the load side. Each parameter can be expressed in an integrated form (Fig. 2). By analyzing loss parameters such as these and considering the results, an estimation can be made of the amount of energy that can be supplied to the load and the system load and power generation capacity can be designed.

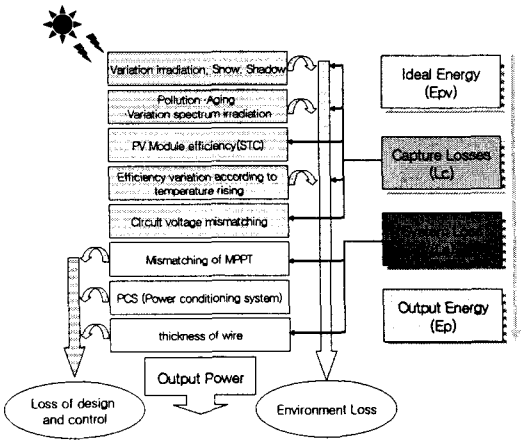

Fig. 2. Block diagram of design parameters

2.2 Performance index of the PV system

To calculate amount of energy yield for a certain proposed PV system, it should be possible to predict the yield from standard performance. Actual energy yield is determined through a comparison between predicted energy yield and performance ratio. Loss parameters existing throughout the entire system should be particularly noted upon analysis of an operating system or the design of a new system. An index representing the performance of a PV system is final energy yield Y_F. When denoting the system output watt-hour as E_{PV}([kWh]), and the design capacity of PV array as P_p([kWp]), the final energy yield expressed in a ratio against E_{PV} ([kWh]) is as shown in equation (1).

$$Y_F = \frac{E_{PV}}{P_p} \tag{1}$$

When the duration of sunshine Y_R(h) is given with the insolation rate $H_A$of an inclined plane on the surface of a PV array, and the standard test condition (STC) G_{STC} is represented as 1[kW/m²], the estimation formula of standard energy is as shown in Equation (2).

$$PR = \frac{Y_F}{Y_R} \tag{2}$$

A performance ratio (PR) is often used for system technical quality (STQ), and performance evaluation can be conducted through comparison of an independently grid-linked system from the installation location, installed tilt angle, standard, and rated output. This is shown in Equation (3).

$$Y_R = \frac{H_A}{G_{STC}} \tag{3}$$

Conducting a performance evaluation through a comparison of an independently grid-linked system from the installation location, installation angle, and rated output, then, gives the final performance ratio from equation (3) as shown in equation (4).

$$Q = PR = \frac{Y_F}{Y_R} = \frac{E_{PV}/P_p}{H_A/G_{STC}} = \frac{E_{PV} \times G_{STC}}{P_P \times H_A} = \frac{\eta_{SYS}}{\eta_{STC}} \tag{4}$$

Actual system efficiency is represented with a multiplication of system loss expressed with component efficiency. This is shown in equation (5).

$$\eta_{SYS} = \eta_{STC} \times \eta_{RRC} \times \eta_{DEG} \times \eta_{SHA} \times \eta_{OMM} \times \eta_{INV} \tag{5}$$

Here, η_{STC} is defined as 1[kW/m²], It means a state of sunlight at the temperature of 25[℃], AM 1.5 spectrum, and slope angle of 0[°], the η_{RRC} of realistic reporting conditions refers to motion condition (not STC of a PV module contributing to the loss amount from the insolation rate and temperature conditions), η_{SHA} means loss caused by shadow on the array, η_{OMM} means loss by voltage discord between strings, and η_{INV}means average inverter loss.

3. Optimum design of the PV system

To analyze the effects of loss factors to ensure the optimum design of a PV system, loss due to the wiring of the array, voltage drop, shadows, azimuth and tilt angle, and junction box should be studied.

3.1 Module and array

For the number of serially connected sheets in the array, the number of serially connected sheets

is found from the value calculated by dividing the 10[%] added voltage of the inverter's normal rated voltage with the maximum output of working voltage. Construction of the array should be designed for improved power generation efficiency through a review of serial and parallel connection methods. Fig. 3 shows a string wiring method. This shows that when a shadow occurs in each string, it affects voltage generation in the whole string. Comparing this with Fig. 3(b), output reduction is clear. In Fig. 3(b), a shadow effect occurs in one string, and causes the whole current to decrease. The voltage is, however, maintained, and the output reduction is small as compared with Fig. 3(a). Therefore, a method of serial connection in the direction of the appearing shadow would enhance efficiency, but output loss can be reduced only when design considers the method of connection as shadow direction varies.

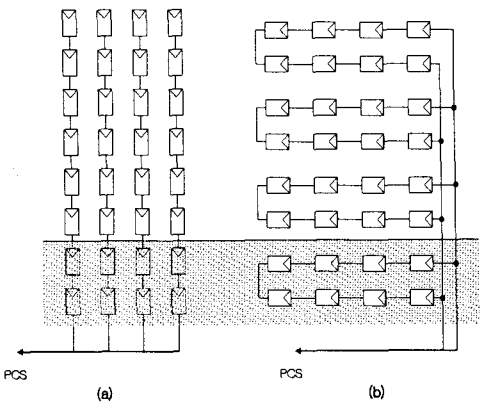

(a) Effect of whole array by shadow
(b) Partial effect by shadow

Fig. 3. Shadow effect of the string

3.2 Loss by voltage drop

The calculation of voltage drop is divided into an informal calculation method and a formal calculation method. In the PV system producing minute power, the informal calculation method calculating the value contains a large error when compared with the actual value, and conformity with other systems such as the inverter is lost, which results in greater system loss. Therefore, the formal method of calculation was utilized. At present, the voltage drop calculation formula applied in actual work mostly utilizes informal calculation, but a difference remains between the informal and the formal calculation formula. The voltage drop calculation formula is shown in Equation (6).

$$\triangle e = K_w \cdot Z \cdot I \cdot L \tag{6}$$

Here, $Z = R\cos\theta + X\sin\theta$, K_ω = single- phase 2-line style: 2, single-phase 3-line style, 3-phase 4-line style: 1, 3-phase 3-line style: $\sqrt{3}$. Denoting a coefficient that can convert line impedance Z into section area S as Hcc, and obtaining the voltage drop $\triangle e$ yields equation (7).

$$\triangle e = H_{cc} \cdot \frac{L}{1000S} \cdot K_w \cdot I \tag{7}$$

For greater efficiency, a flowchart for thickness selection of main line was suggested in Figure 4.

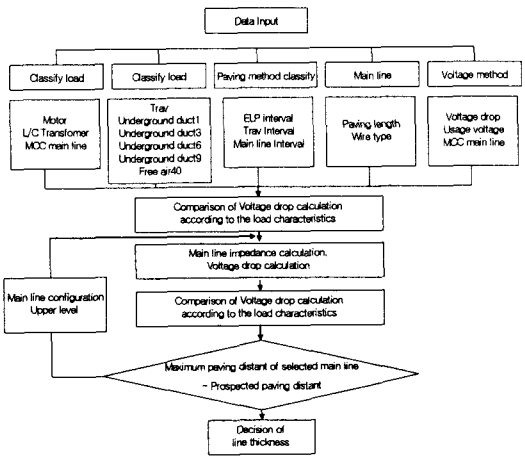

Fig. 4. Flowchart for thickness selection of main line

3.3 Shadow effect

Most PV systems are affected by shadow for a certain time or partially during the day. Shadows frequently arise especially over PV arrays installed in urban areas. This is particularly the case in winter. Factors include altitude of the sun, the size and shape of nearby buildings, and obstacles such as tree.

Generally, since the altitude of the sun is higher in summer, the effect of shadows is less. The effect of shadows increases just before sunset in winter. This loss appears in the range from approximately 5[%] to at most 20[%], and depends upon the structure of the array or site. Fig. 5 defines angles for the calculation of separation distance between arrays. Calculation of separation distance to avoid the effect of shadows between arrays is found with Equation (8).

$$d/a = \cos\beta + \frac{\sin\beta}{\tan\varepsilon} \tag{8}$$

Here, $\varepsilon = 90^\circ - \delta - \phi$, a : module length, d : separation distance, β: tilt angle of module, ε: angle of elevation. Shadow angle is based on azimuth angle when it is 12:00 at the winter solstice[5-6].

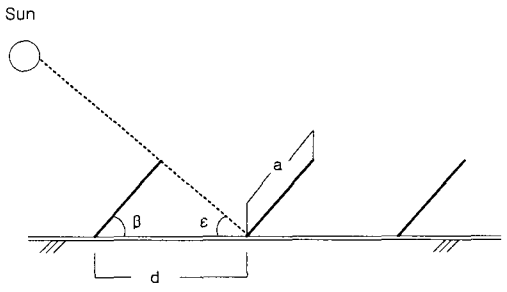

Fig. 5. Separation distance of the array

3.4 Loss by azimuth and tilt angle

Generally the azimuth of the array in a solar cell is due south, namely '0' degrees, at which the generation wattage per unit capacity of solar cell becomes maximal. Here, when the area for installation is limited, this angle is selected so that a maximum generation of output can be obtained when daily generation is maximal or where the load side is maximal through the selection of an angle that can avoid the azimuth angle of a roof or land, or the shadow of a mountain, hill or building. To ensure the peak generation rate coincides with the time when the load peaks through the adjustment of the azimuth angle, selection of the azimuth angle depends upon Equation (9).

Azimuth angle
= (time of maximum load during a day12)
× 15 + (longitude in installation area standard time longitude) (9)

The tilt angle of the array should be selected so that generation wattage of the array in solar cell is normally maximal. When utilizing a roof where an incline already exists, the tilt angle of the roof is selected. In areas with a large amount of snowfall, a tilt angle enabling the snow to slide off is selected. Here, the tilt angle enabling snow to slide off is about 50~60[°].

3.5 Junction box

The junction box is installed where maintenance and inspection can be performed easily, for the purpose of making an orderly junction of plural solar cell modules, making inspection easy through circuit separation upon maintenance and inspection, and minimizing the range of stops when issues arise in the array of the solar cell. The junction box is constructed of direct current output switchgear, a lightning element, back-current prevention and a terminal box. The

switch for output and short-circuits is installed for confirmation of short-circuit current upon measurement of insulation resistance and regular inspection. Fig. 6 shows a circuit diagram of the junction box.

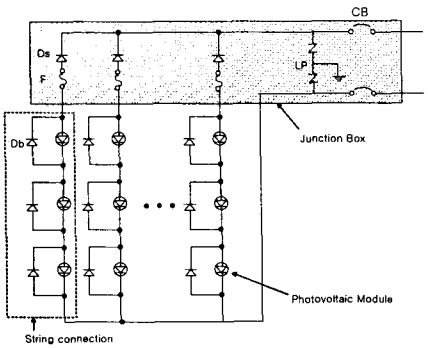

Fig. 6. Circuit diagram of the junction box

4. Results of the simulation and experiment

4.1 Module and array

The simulation parameters of the 10[kW] PV system were: longitude of 126.55[°], latitude of 35.8[°], tilt angle of 30[°], and azimuth of due south. Two arrays were constructed of 17 series x 4 parallels with a 75W solar cell module. Table 1 shows the parameters of the module.

In the junction method proposed in this paper,under the parameters shown in Table 1, the array was constructed so that each serial-junction module within a parallel-connection module was not affected by shadow. The spacing between the arrays was designed based on 09:30~15:30 when insolation strength and inverter conversion efficiency is satisfactory while the effect of shadow is the largest to the maximum based on the winter solstice. The simulation was performed using the formal calculation method in the design of the voltage drop[7-8].

Table 1. Parameter of module

Parameter	Value	Parameter	Value
Pmax(W)	75	Cell Size(mm)	125×125
VOC(A)	21.80	Efficiency([%])	10.20
ISC(A)	4.75	Module Size(mm)	1204×537
Vm(V)	17.30	Module Quantity(ea)	136
Im(A)	4.35	Array(series×parallel)	17×8

Fig. 7(a) indicates a power characteristic curve following the characteristics of output voltage and current of the existing system, while Fig. 7(b) shows the simulation result of the power characteristic curve following the characteristics of output voltage and current of the proposed system.

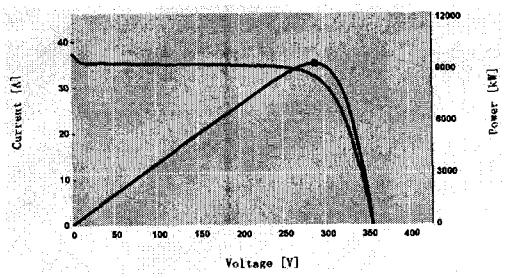

(a) PV system of the existing mode

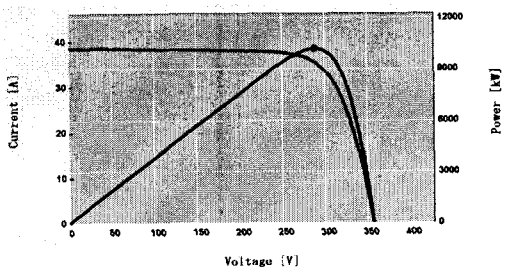

(b) PV system of the proposed mode

Fig. 7. I-V characteristics of the PV system

4.2 Loss by voltage drop

Voltage drop is designed mainly with an

informal design mode. Loss for both the informal and formal design modes was estimated through the simulation.

Table 2 indicates voltage drops by capacity of the 3-phase grid-linked inverter. When the voltage drop is calculated following the formal design mode proposed in this paper, a difference of around 0.31[%] was exhibited compared with the existing informal design mode. The voltage drop difference following the supply mode of the main line was exhibited to be around 1.05[%].

This indicates that the AC supply into the main line of the 3-phase inverter has less voltage drop than the DC supply. Since wire loss should also be taken into account, the inverter should be installed as closely as possible to the array.

Table 2. Comparison of voltage drop of the inverter

Capacity	Voltage drop rate of DC supply[%]		Voltage drop rate of AC supply[%]	
	formality calculation	simplicity calculation	formality calculation	simplicity calculation
10[kW]	1.63	1.32	0.58	0.47
20[kW]	2.05	1.65	0.74	0.60
30[kW]	1.84	1.44	0.64	0.51
50[kW]	2.03	1.52	0.69	0.53
100[kW]	2.60	1.80	0.86	0.61

Fig. 8 indicates voltage drop rates calculated with both the informal and formal calculation modes for drop rates when the main line is supplied with DC power for each capacity. In the formal calculation mode, a difference of around 0.3 ~0.82[%] appeared in the voltage drop rate. It can be said that a difference in voltage drop rate appears largely as the capacity becomes larger.

Fig. 9 indicates voltage drop rates calculated with both an informal and formal calculation mode for drop rates when the main line is supplied with AC power for each capacity. In the formal calculation mode, a difference of around 0.11~ 0.25[%] appeared in the voltage drop rate. It can be said that a difference in voltage drop rates appears largely as the capacity becomes larger, but the difference is less in the case of DC supply.

Fig. 10 indicates voltage drop rates calculated with both an informal and a formal calculation mode for drop rates the when main line is supplied with DC and AC power for each capacity. Fig. 11 indicates voltage drop rates calculated with both an informal and a formal calculation mode for AC supply. It can be said that the voltage drop rate appears less for the DC power supply mode than for the AC power supply mode.

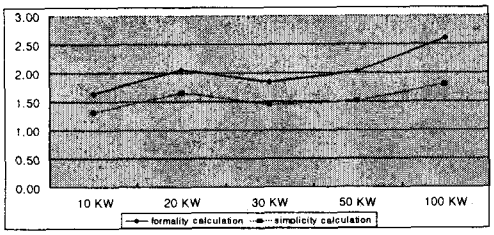

Fig. 8. Voltage drop following the DC voltage

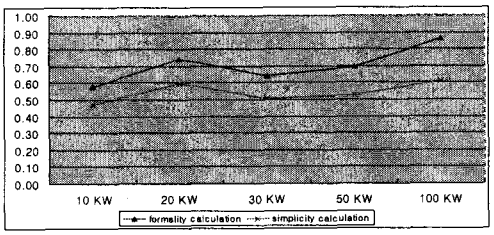

Fig. 9. Voltage drop following the AC voltage

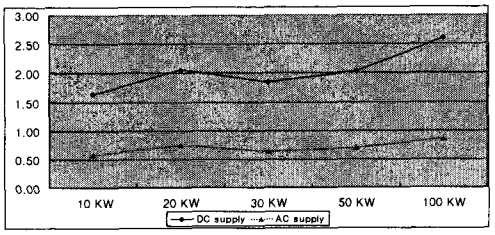

Fig. 10. Voltage drop following the formal calculation mode for drop rates

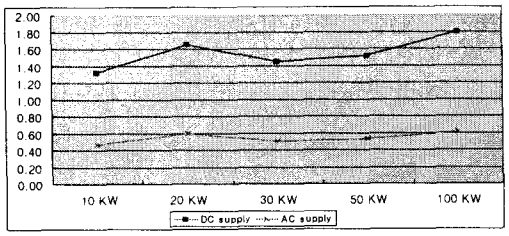

Fig. 11. Voltage drop following the informal calculation mode for drop rates

4.2 Loss by shadow

Time simulation in the installation area was based on a time of 9:30 at the winter solstice following the separation distances in Table 3 and 4. The effects of shadow are as shown in Fig. 12. Consideration of the existing shadow effect was applied based on the altitude at 12:00 at the winter solstice. For the angle of elevation proposed in this paper, however, the separation distance was calculated based on the altitude when it is 9:30 at the winter solstice.

Table 3. Altitude and angle of elevation of the sun at 12:00

Area	Latitude ([°])	Altitude and angle of elevation of the sun([°])	Tilt angle ([°])	Separation distance
Seoul	37.30	28.3	30	1.79 × a
Daejeon	36.20	29.5	30	1.74 × a
Gwangju	35.09	30.5	30	1.71 × a
Jeju	33.30	32.3	30	1.65 × a

Table 4. Altitude and angle of elevation of the sun at 9:30

Area	Latitude ([°])	Altitude and angle of elevation of the sun([°])	Tilt angle ([°])	Separation distance
Seoul	37.30	15	30	2.7 × a
Daejeon	36.20	16	30	2.6 × a
Gwangju	35.09	17	30	2.5 × a
Jeju	33.30	18	30	2.4 × a

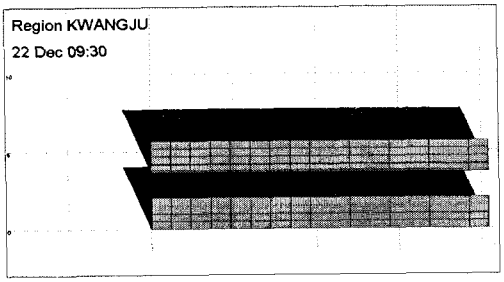

(a) Effect of shadow at 12:00

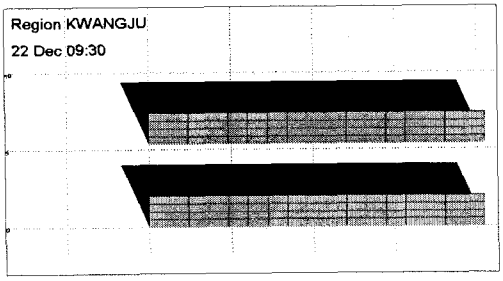

(b) Effect of shadow at 9:30

Fig. 12. Effect of shadows following the separation distance

When the separation distance caused by the shadow effect was calculated in the proposed mode, the effect of shadow was slightly smaller at 9:30 than for the existing 12:00 standard. The generation rate was therefore improved by about 3[%]. When the separation distance was set based on 9:30, it was not affected by shadow when it was based on 12:00, it was found that shadow occurs in the array module at sunrise and sunset, causing a possible reduction in efficiency. The effect of shadow was particularly noticeable in winter and therefore a difference in power generation rate was exhibited.

4.3 Loss by tilt angle

Performance of the 10[kW] grid-linked system was simulated using system parameters. In Fig. 5, the yearly power generation rate following the tilt angle of the system was compared and analyzed.

It was measured up to 90[°] at 5[°] elevation increments, and the power generation rate of the system was compared using a vertical tracer. Among the fixed angles, the highest power generation rate was exhibited at a tilt angle of 30[°], and the system using the vertical tracer exhibited a power generation rate 107[%] higher than the system having a fixed angle of 30[°]. It could be said that over 95[%] of the maximum power generation rate was exhibited in the system having a fixed angle from 10[°] to 55[°], and therefor no significant difference appeared.

4.4 Result of the experiment using the proposed design technique

To compare and analyze performance characteristics of the PV system for the purpose of an optimum design for improving the efficiency of the PV system, Fig. 13 shows monthly output wattage of the PV array during the analysis period from November 2005 to October 2006.

Owing to weather conditions such as snowfall in winter, the case in which the operation of the PV system stops also in a state of good insolation condition occurs frequently. Since weather conditions (snowfall) were particularly poor in January, the power generation rate was significantly lower than in November, December, and February. Also, since there were many days of good insolation in March, the power generation rate appeared the most high. As weather condition and insolation rate was also good in August, September, and October, the power generation rate was high. In July, however, the operation rate of the PV system was over 40[%], but by comparing it with other months, the output wattage decreased owing to a decrease of the insolation rate in general which determines power generation performance, due to poor weather conditions (cloud, rainfall, temperature change, etc.), and an increased loss of the PV array due to temperature rise. This was shown as a graph in Fig. 13.

Table 5. Power generation rate of the PV following the tilt angle

Angle	Year Wh	Month Wh	Day Wh	Ratio
0	11,750,397	979,200	32,193	89.6[%]
5	12,168,099	1,014,008	33,337	92.8[%]
10	12,508,457	1,042,371	34,270	95.4[%]
15	12,771,373	1,064,281	34,990	97.4[%]
20	12,957,036	1,079,753	35,499	98.8[%]
25	13,069,612	1,089,134	35,807	99.7[%]
30	13,114,082	1,092,840	35,929	100.0[%]
35	13,098,056	1,091,505	35,885	99.9[%]
40	13,033,561	1,086,130	35,708	99.4[%]
45	12,923,109	1,076,926	35,406	98.5[%]
50	12,759,319	1,063,277	34,957	97.3[%]
55	12,539,744	1,044,979	34,355	95.6[%]
60	12,261,549	1,021,796	33,593	93.5[%]
65	11,920,134	993,345	32,658	90.9[%]
70	11,519,723	959,977	31,561	87.8[%]
75	11,067,344	922,279	30,321	84.4[%]
80	10,561,267	880,106	28,935	80.5[%]
85	9,998,487	833,207	27,393	76.2[%]
90	9,385,347	782,112	25,713	71.6[%]
Ver. Tr	14,028,360	1,169,030	38,434	107.0[%]

Fig. 14 is a characteristic graph for the monthly inverter conversion efficiency of the PV system. As yearly average efficiency of the existing system is 90.32[%], and yearly average efficiency of the proposed system appeared to be 91.11[%], there was a difference in inverter efficiency. Fig. 15 indicates the conversion efficiencies of the array. During the analysis period, the average conversion efficiency of the existing PV system was 9.39[%], while the efficiency of the proposed system was 9.62[%]. Since the module charac-

teristic of the proposed system for temperature was good, the conversion efficiency was also improved. As a result of data analysis, when the insolation rate is lowered, the conversion efficiency of the array in the solar cell was lowered, and when it decreased below 30[%] of the rated output, the inverter efficiency also decreased significantly. Therefore, it was confirmed that the various efficiencies of the system as a whole were lowered all.

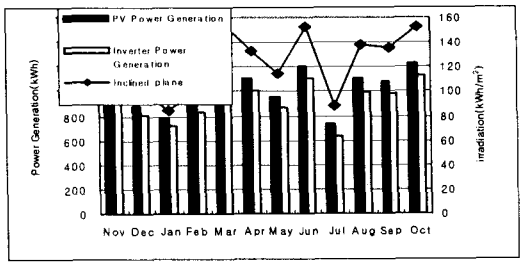

(a) The proposed PV system

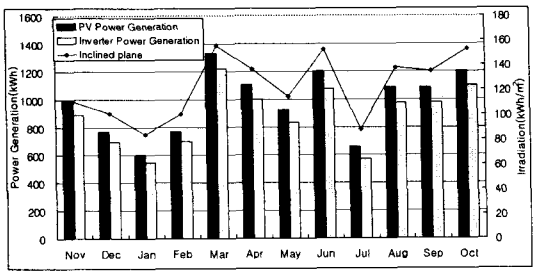

(b)The existing PV system

Fig. 13. Output characteristic following the varied insolation rate

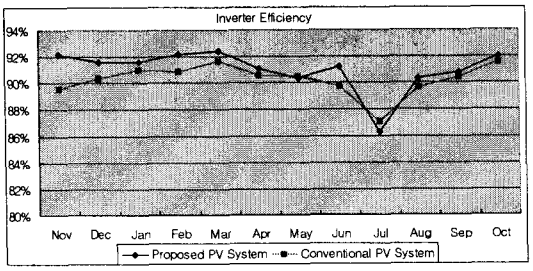

Fig. 14. Monthly inverter efficiency

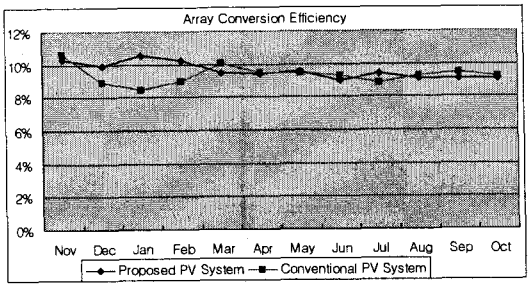

Fig. 15. Monthly array conversion efficiency

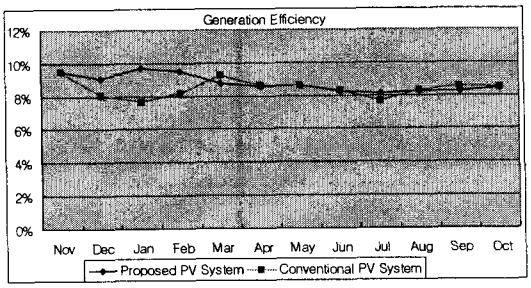

Fig. 16. Monthly system power generation efficiency

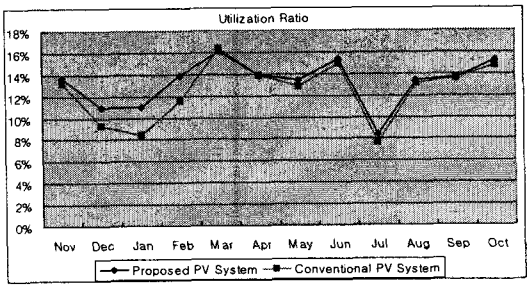

Fig. 17. Monthly system use rate

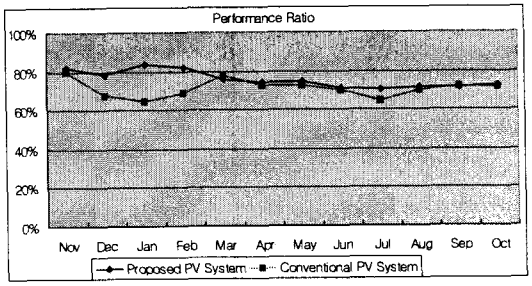

Fig. 18. Monthly performance ratio

Fig. 16 indicates the monthly system power generation efficiency of the PV system, while Fig. 17 indicates the characteristics of system use rate. During the analysis period, for the system power generation efficiency of the PV system, the existing system exhibited 8.48[%], and the proposed system was 8.67[%]. The efficiency of the proposed system improved slightly. Regarding use rate, the existing system was 12.51[%], and the proposed system was 13.23[%]. The proposed system showed slight improvement for this, as well.

The performance ratio, which is an important analysis item in evaluating and analyzing the performance of the component parts of the PV system and whole system as well as loss factors of the PV system, was shown in Fig. 18. During the analysis period, the performance ratio of the existing system was 71.24[%], while the performance ratio of the proposed system was 74.89[%].

5. Conclusion

In this paper, an optimum design that considers external environment conditions, the array construction of solar cells, PCS, and installation conditions was targeted for the improvement of efficiency of a 10[kW] PV system. The proposed design mode was applied to a 10[kW] grid-linked PV system using a simulation. By studying the operational characteristics and system stability following the array features of the solar cell, PCS characteristics, system efficiency and system performance through an operational demonstration of the system, the feasibility of the optimum design mode proposed through the analysis was reviewed.

As a result of studying the optimum design mode for the improvement of efficiency of the PV system through consideration of loss parameters, a mode that approaches a systematic loss compensation method was proposed. It is feasible that this mode will be useful for the field of photovoltaic power generation business as it can play an important role in the field of renewable energy by means of developing a better loss compensation mode.

In the future, more research should be done to establish high efficiency energy conversion systems by means of devising more detailed design modes regarding loss factors.

Acknowledgement

This work was supported by the Korea Research Foundation Grant funded by the Korean Government (MOEHRD), No.R05-2004-000-10893-0

References

[1] K. Konno, Y. Fujisawa, "Experiences in Field Test Programs of Japan", 9th International PVSEC, 1996, pp493-495.
[2] Tomas Markvart, "Solar Electricity", John Wiley & Sons, pp. 37, 2002.
[3] 山田興一, 小宮山宏, "太陽光發電工學", 日經 BP社, pp. 164~165, 2002.
[4] A.Goetzberger, V.U.Hoffmann, "Photo -voltaic Solar Energy Generation", Springe, pp.113~283, 2005.
[5] KEMCO, Kepri, electric power lab., "A study of the system evaluation and optimization for the PV system in the Inhibited island", Korea Electric Power Research Institute , 1999.5.
[6] Renewable energy center "Standards of the Installation and Construction for the New&Renewable energy ", KEMCO, 2005.
[7] Nagayoshi, H., Orio, S., Kono, Y., Nakajima, H., "Novel PV array/module I-V curve simulator circuit" IEEE Photovoltaic Specialists Conference 2002 , pp1535-1538 , 2002. 5.
[8] N Kasa and T Iida, H Iwamoto, Maximum Power Point Tracking with Capacitor Identifier for Photovoltaic Power System, IEE, 2000, pp.130-135.

Biography

Kang-Yeon Lee

1997: Graduated from the Department of Electrical Engineering, the College of Engineering, Chosun University. 1999: Graduated from the Department of Electrical Engineering, the Graduate School of Chosun University (Master's degree). 2004: Graduated from the Department of Electrical Engineering, the Graduate School of Chosun University (Ph.D., engineering). 2005~ at present: Adjunct faculty of Chosun University.

Moon-Han Choi

1990: Graduated from the Department of Electrical Engineering, the College of Engineering, Chosun University. 1999: Graduated from the Department of Electrical Engineering, the Graduate School of Industry, Chosun University (Master's degree). 2007: Graduated from the Department of Electrical Engineering, the Graduate School of Chosun University (Ph.D., engineering). 2004~ at present: CEO, Kiram Engineering Co., Ltd. Professional engineer for electrical facilities of building ('98). Double-post professor in the Department of Electrical Engineering, Chosun University.

Youn-Ok Choi

1995: Graduated from the Department of Electrical Engineering, the College of Engineering, Chosun University. 1997: Graduated from the Department of Electrical Engineering, the Graduate School of Chosun University (Master's degree). 2003: Graduated from the Department of Electrical Engineering, the Graduate School of Chosun University (Ph.D., engineering). 2006~ at present: Research professor in the Department of Electrical Engineering, Chosun University.

Byeong-Ho Jeong

1997: Graduated from the Department of Engine Science, Yeosu University. 1999: Graduated from the Department of Electrical Engineering, the Graduate School of Chosun University (Master's degree). 2006: Graduated from the Department of Electrical Engineering, the Graduate School of Chosun University (Ph.D., engineering). At present: Head researcher, Annex Research Center, Kiyoung Midas Co., Ltd.

Geum-Bae Cho

1980: Graduated from the Department of Electrical Engineering, the College of Engineering, Chosun University. 1982: Graduated from the Graduate School of Chosun University (Master's degree). 1995: Graduated from the Department of Electrical Engineering, the Graduate School of Konkuk University (Ph.D., engineering). 1966~1987: Guest researcher, Univ. of Oklahoma, OK, USA. 1998~1999: Visiting exchange professor, Oregon State Univ., OR, USA. At present in 2007: Professor in the Department of Electrical Engineering, Chosun University.